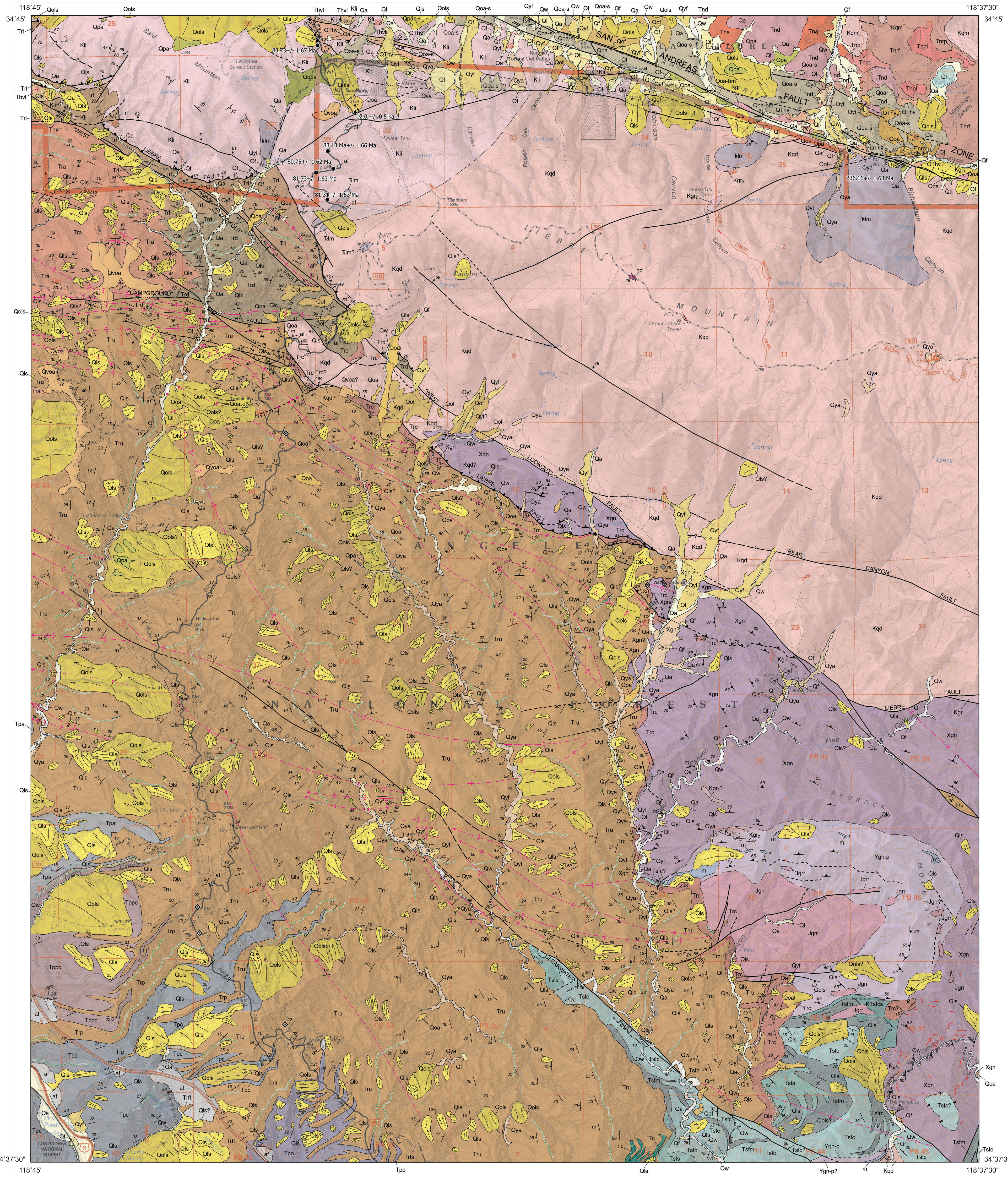

Coordinate System:
Universal Transverse Mercator, Zone 11N
North American Datum 1927

Topographic base from U.S. Geological Survey
Liebre Mountain 7.5-minute Quadrangle, 1958, photo revised 1988.
Shaded relief image derived from USGS Lidar DEM, 2017

Scale 1:24,000

Contour Interval 40 Feet
Dotted Lines Represent 20-Foot Contours
Contour Interval on River Surface 5 Feet
National Geodetic Vertical Datum of 1929

Approximate Mean Declination, 2023

This geologic map was funded in part by the USGS National Cooperative Geologic Mapping Program, STATEMAP Award no. G22AC00356.

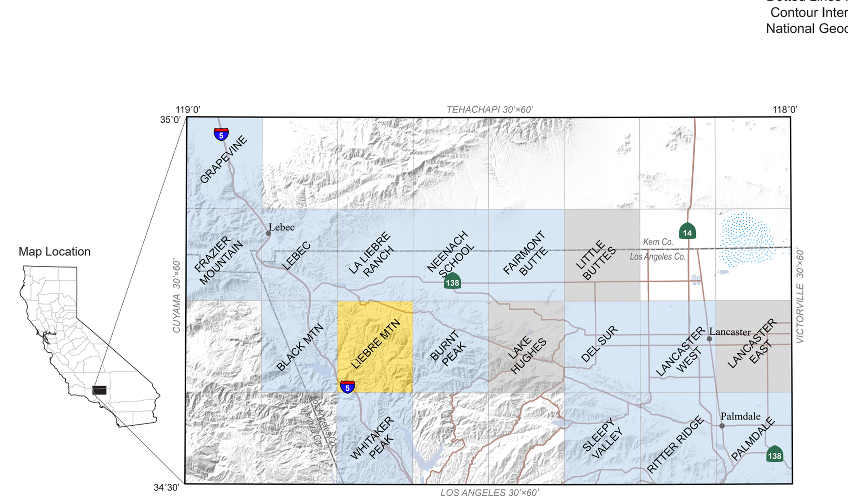

Liebre Mountain 7.5-minute Quadrangle

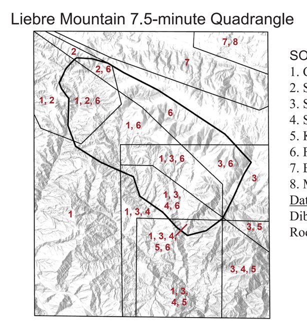

SOURCES OF MAP DATA
1. Crowell 1982
2. Sexton, 1990
3. Szatai, 1961
4. Smith, 1951
5. Kooser, 1980
6. Faggioli, 1952 (Map area outlined)
7. Barrows and others, 1985
8. Matthews, 1973

Data sources that cover entire quadrangle:
Dibblee, 2002
Rodriguez and Swanson, 2023

Professional Licenses and Certifications:
F. N. Rodriguez - PG No. 10171
B. J. Swanson - PG No. 9494, CEG No. 2055

Signature, date, and stamp of licensed individual's seal found within the accompanying document: Authorship Documentation and Product Limitations.

Publication Title: "Preliminary geologic map of the Liebre Mountain 7.5' Quadrangle, Los Angeles County, California: California Geological Survey Preliminary Geologic Map 23-02, scale 1:24,000".

PRELIMINARY GEOLOGIC MAP OF THE LIEBRE MOUNTAIN 7.5' QUADRANGLE LOS ANGELES COUNTY, CALIFORNIA

VERSION 1.0

By
Francesca N. Rodriguez & Brian J. Swanson

Digital preparation by
Francesca N. Rodriguez, Brian J. Swanson, Jeremy L. Altringer and Deshawn A. Brown Jr.

2023

Preliminary Geologic Maps available from:
https://www.conservation.ca.gov/cgs/rgm/preliminary

DESCRIPTION OF MAP UNITS

SURFICIAL UNITS

af — **Artificial fill and disturbed areas (Holocene, historic)**—Consists of anthropogenic deposits of earth-fills derived from local sources. Mapped primarily along road alignments and at larger anthropogenic berms.

Ql — **Lake deposits (late Holocene)**—Mostly unconsolidated fine-grained sand, silt, and clay. Deposits may contain salts or other evaporites as well as interfingered alluvium deposited when lake levels are low.

Qw — **Wash deposits (late Holocene)**—Unconsolidated sand, gravel, and cobbles deposited in recently active stream channels. Sediments are generally derived from local bedrock or reworked from nearby older Quaternary deposits. Sediments subject to remobilization and deposition during storm events.

Qf — **Modern alluvial fan deposits (late Holocene)**—Unconsolidated to weakly consolidated, poorly sorted deposits of sand, silt, gravel, and cobbles with locally common boulders, forming active, essentially undissected, alluvial fans. Includes small cones at the mouths of stream canyons, and broad aprons of coarse debris adjacent to mountain fronts. Gravel clasts are derived from local up-slope sources and typically unweathered with little to no oxidation. Sediments subject to remobilization and deposition during storm events.

Qa — **Modern alluvial valley deposits (late Holocene)**—Unconsolidated to weakly consolidated, mostly undissected, sand, silt, gravel and cobbles and local boulders deposited dominantly by fluvial processes. Deposited parallel to localized stream valleys and/or underlying larger river valleys; subject to remobilization and deposition during storm events.

Qpa — **Ponded alluvium (Holocene)**—Unconsolidated to weakly consolidated, moderately sorted and bedded sand and silt with minor gravel ponded upstream of drainages offset by adjacent faults, constricted by landslide movement, or accumulated in closed depressions.

Qls — **Landslide deposits (Holocene to late Pleistocene)**—Unconsolidated to moderately well-consolidated jumbled sediment or rock debris consisting of surficial failures, debris flows, rock avalanches, and large-scale rockslides. Recognizable by topographic expression, such as hummocky terrain, closed depressions, deflected drainages, scarps, chaotic internal structure, pervasive fracturing, or out-of-sequence rock packages.

Qyf — **Younger alluvial fan deposits (Holocene to late Pleistocene)**—Unconsolidated to weakly consolidated, undissected to slightly dissected, light-brownish-gray (10YR 6/3-2) silty and coarse- to very coarse-grained sand with pebbles, cobbles and uncommon boulders; poorly to moderately stratified. Subject to remobilization and deposition during large storm events.

Qya — **Younger alluvium and terrace deposits (Holocene to late Pleistocene)**—Unconsolidated to slightly consolidated, interlayered, yellowish-brown (10YR 5/4) thin- to thick-bedded deposits of sand, gravelly silty sand, and local cobble-rich layers; clasts typically reflect upstream bedrock sources and deposits. Deposits are slightly to moderately dissected by modern streams but could be modified by runoff from large storm events. Deposits in Cienega Canyon contain locally abundant clasts of quartz diorite derived from Liebre Mountain.

Qols — **Older landslide deposit (late to middle Pleistocene)**—Moderately consolidated jumbled rock debris and breccia. Recognizable by topographic expression or chaotic internal structure; Pleistocene age inferred from degree of incision and modification, and cross-cutting relationships.

Qopa — **Older ponded alluvium (late to middle Pleistocene)**—Moderately consolidated, moderately sorted, moderately bedded sand and silt with gravel. Ponded upstream of drainages blocked by landslides but are overprinted by moderate incision; topographically higher on slopes than Qpa. Mapped in saddle between Bald and Liebre Mountains where it is ponded by an old landslide.

Qof — **Older alluvial fan deposits (late to middle Pleistocene)**—Light-yellowish-brown (10YR 6/4) fine- to coarse-grained sand deposits with silt, pebbly sand and scattered gravel- and cobble-size clasts. Clasts are subrounded to subangular and generally composed of crystalline basement rock. Qof is slightly to moderately consolidated, poorly sorted and poorly stratified. Surfaces are slightly to strongly dissected; primarily occur on the south flank of Liebre Mountain near the Liebre and "West Lookout" faults and locally along the San Andreas Fault.

Qoa — **Older alluvium (late to middle Pleistocene)**—Dark-grayish-brown (10YR 4/2) silty pebbly sand with coarse subrounded to subangular gravel and local cobbles; clasts composed of locally derived crystalline basement rock; slightly friable to well consolidated, moderately to poorly sorted; weakly stratified to locally well stratified. Surfaces are strongly dissected, and topographically elevated along fault traces and along drainages. Mapped older alluvium likely reflects more than one period of deposition. Well consolidated, moderately well bedded, silty sand Qoa is cut by an unnamed fault splay northwest of Cold Canyon; origin of the perched deposit may be related to old landslide mapped to northwest; this faulted alluvium was dated at 12.0 +/-0.55 ka (one sigma error reported; IRSL analysis on K-feldspar in 2020 by Shannon Mahan at USGS Luminescence Lab, written commun.).

Qoa-bm — **Boulder gravel of Bald and Liebre Mountain (late Pleistocene)**—Brown (10YR 4/3) unconsolidated, poorly sorted, very coarse pebble- to boulder -size, subangular to subrounded clasts generally ranging up to 0.75 meters in diameter, and locally up to 2 meters in diameter. Clasts consist of granite, quartz diorite, granodiorite, potassium feldspar megaporphyry, and diorite, which are derived primarily from Liebre Granodiorite and Quartz Diorite (Kli), Triassic megaporphyry (Trlm), and granites exposed south of the San Andreas Fault, or from Qoa-s (Barrows and others, 1985).

Qoa-s — **Old alluvium ["Sandberg Formation" of Barrows and others, 1985] (late Pleistocene)**—Brown to dark-yellowish-brown (10YR 4/3 to 4/4), poorly sorted gravel, breccia, and sand with local light-gray silty sand layers in a gray to red earthy matrix. Discontinuously and irregularly bedded to locally moderately bedded to locally massive with dispersed, variable iron-oxide staining. Clasts consist of angular to subangular cobbles and pebbles derived exclusively from the Liebre Granodiorite and Quartz Diorite (Kli) of Bald and Liebre Mountains. Basal conglomerate layer contains well-rounded, intensely weathered cobbles and boulders of granite, aplite/fine-grained leucogranite, diorite, megaporphyry, and local mafic lithologies of rock in an earthy to sandy matrix (Barrows and others, 1985). Mapped as "Sandberg Formation" by Barrows and others (1985) for exposures north of Sandberg. Mapped distribution of Qoa-s suggests an association with underlying or up-gradient basement-involved landslide deposits. Western exposures mapped by Ramirez (1984) reportedly contain more diverse clast assemblages, specifically including marble boulders. Tilted and uplifted along the San Andreas Fault.

Qvoa — **Very old alluvium (early Pleistocene)**—Silty, fine- to coarse-grained sand and gravel derived from crystalline bedrock; moderately to well-consolidated, highly dissected. Topographically located on high ridgelines with original alluvial surface degraded due to erosion.

SEDIMENTARY ROCKS OF RIDGE BASIN GROUP

The portion of the Ridge Basin Group exposed in the Liebre Mountain Quadrangle is comprised of four interrelated, late Miocene to Pliocene stratigraphic units: the basal marine Castaic Formation, which is overlain by fine-grained lacustrine deposits of the Peace Valley Formation near the basin axis that interfinger with the deltaic and fluvial deposits of the Ridge Route Formation. This sequence is overlain by the fluvial and floodplain deposits of the Hungry Valley Formation (Crowell, 2003b).

Hungry Valley Formation (early Pleistocene to late Miocene)—The type-section for the nonmarine Hungry Valley Formation is located near Freeman Canyon in the Lebec Quadrangle northwest of the map area, with an approximate maximum thickness of 1,500 m. Depositional environments for these sediments were dominantly fluvial to alluvial floodplain environments with local overbank deposition (Loeffler and Bennett, 1990). Paleocurrent data and exotic clast composition indicate the majority of the sediments composing this unit were derived from elevated terrain to the north or northeast of the basin, which is now displaced to the southeast by the San Andreas Fault (Link, 1982c; 1983; 2003; Ramirez, 1983; 1984; Weldon and others, 1993; Cohen, 2016).

QThv — **Hungry Valley Formation, undifferentiated (early Pleistocene to late Miocene)**—White to gray; poorly to moderately cemented; locally well-indurated; well-bedded to irregularly bedded and massive; poorly to moderately sorted; nonmarine, fine- to coarse-grained arkosic sandstone and pebble to cobble conglomerate interbedded with reddish to greenish-gray, well-bedded to massive micaceous, silty sandstone and shale. Equivalent to "Th" mapped by Barrows and others (1985).

QThvu — **Hungry Valley Formation, upper member (early Pleistocene to late Pliocene)**—Nonmarine, massive breccia-conglomerate in a yellowish-brown (10YR 5/4) to very pale brown (10YR 8.5/2) silty sand matrix, interbedded with crudely bedded pebbly to cobbly sandstone and poorly bedded, poorly sorted, light-brown pebbly to cobbly sandy mudstone. Moderately to locally well bedded with 5 to 10 cm thick fine-grained sandstone and conglomerate beds. Poorly exposed along Pine Canyon Road, except where lying unconformably on top of the Neenach Volcanics in a road cut; unconformably overlain by Qoa-s. Clasts are subrounded to subangular and range in size up to small boulders; clast types consist primarily of granite, diorite, quartz diorite, gneiss, marble, schist, quartzite, and gneiss; volcanic rock of the Neenach Volcanics occur at the base where it is in depositional contact. Equivalent to unit "Thu" by Barrows and others (1985).

Thvl — **Hungry Valley Formation, lower member (Pliocene to late Miocene)**—Nonmarine, white to gray to buff, subangular, fine- to very-fine-grained, well-indurated, moderately to well-sorted, pebbly arkosic sandstone with coarse- to very coarse-grained conglomerate breccia layers locally common. Sandstone beds exhibit both planar and trough cross bedding, channel scour-and-fill structures, and local clast imbrication. According to Barrows and others (1985), some exposures south of the San Andreas Fault overlying the basement consist almost entirely of very coarse-grained massive arkosic sandstone, mapped by Barrows as "Tha", which is included herein as part of Thvl. The Thvl is overlain by the undivided QThv, and rests either unconformably over the Liebre granodiorite and quartz diorite (Kli), or conformably overlies the Ridge Route Formation, with the contact being interfingering or gradational (Weber, 1988).

Ridge Route Formation (late Miocene)—The Ridge Route Formation is composed primarily of terrestrial, deltaic, and shallow lacustrine/shoreline facies. Deposition occurred in shallow subaqueous to terrestrial environments grading from southwest to northeast, representing three primary facies: shoreline, fluvial and alluvial fan from the basin axis to crystalline bedrock source areas to the northeast (Link, 1982b); grain-size increases to the northeast toward the basin margin and paleocurrent data indicates sediments were derived from the northeast (Link, 1982c); stromatolites locally occur in the shoreline facies (Link, 1978) and selected localities are shown on the map. Sandstone fingers that extend to the southwest all the way to the basin axis are formally named members where they are separated by members of the Peace Valley Formation but are lithologically indistinguishable from strata on strike to the northeast within undifferentiated portion of the Ridge Route Formation (Tru), and are therefore separated using a gradational transition contact symbol on the map. Four of the five formally defined members of the Ridge Route Formation (Link, 1982a) are exposed within the Liebre Mountain Quadrangle: Fisher Spring Sandstone (Trfs), Frenchman Flat Sandstone (Trff), Piru Gorge Sandstone (Trp), and Apple Canyon Sandstone (Tra). Three informal members are also present within the map area as defined by two thesis studies: Liebre sandstone (Trl) (Sexton, 1990), Deer Canyon sandstone (Trd) (Sexton, 1990), and the Cold Canyon conglomerate (Trc) (Faggioli, 1952).

Tru — **Ridge Route Formation, undifferentiated** —The "undifferentiated" designation is used where boundaries between members are not defined northeast of the interleaved, finer-grained Peace Valley Formation members, following the convention used by Crowell and others, 1982. Along the northeastern margin of the basin, Tru contains gravel- to cobble-size, poorly stratified well-rounded to angular clasts composed dominantly of highly weathered granitic clasts with subordinate volcanic, quartzite, metamorphic and sandstone clasts derived from older units to the northeast (Link, 1982b); stromatolites and vertebrate fossils locally observed near Old Ridge Route (see map). Primarily consists of light yellowish-brown (10YR 6/4) silty sandstone with lesser sandy siltstone (Faggioli, 1952). Resistant, continuous sandstone beds were selectively mapped as marker beds within the unit based on interpretation from aerial imagery or lidar. Tru locally unconformably overlies gneissic basement along Cienega Canyon.

Trl — **Ridge Route Formation, Liebre sandstone member**—The Liebre sandstone was initially informally defined as a formation by Faggioli (1952) for exposures of sandstone and conglomerate beds in the headwaters of Liebre Gulch; Sexton (1990) subsequently informally re-defined this as a member of the Ridge Route Formation. This informal member consists primarily of light-gray to light-yellowish-gray sandstone pebbly sandstone and conglomerate with local interbeds of light olive-gray mudstone and poorly sorted muddy sandstone (Faggioli, 1952). Clasts are typically subangular to subrounded and composed dominantly of light pinkish-gray granite of uncertain affinity and subordinate but locally abundant biotite-rich quartz diorite likely sourced from the adjacent basement rock at Liebre Mountain. This unit represents terrestrial basin margin deposits that are heavily interfingered with basinal deposits of the Apple Canyon Sandstone (Tra) to the south and southwest. Conglomerate beds are up to 3 m thick, matrix supported with a fine-grained sandstone matrix, and contain subangular to subrounded clasts up to 50 cm. Freshwater stromatolites are locally found along this transition supporting the interpretation of a nearshore depositional environment.

Trd — **Ridge Route Formation, Deer Canyon sandstone member**—The Deer Canyon sandstone member originally proposed as a formation by Faggioli (1952) who defined the type-section of this unit along the south-facing cliffs directly north of the Tumble Inn Campground; Sexton (1990) reduced it to member status. Trd consists of dark-yellowish-orange resistant beds of coarse-grained sandstone and pebble conglomerate. Conglomeratic sandstone is pale-orange and yellowish-gray to dark-yellowish-orange, fine- to coarse-grained, poorly sorted, subangular to subrounded pebble- to cobble-sized clasts with long axes commonly oriented parallel to bedding. Exposures of this unit are located on the east side of Liebre Gulch between the informal "West Lookout" Fault and the "Campground" Fault (Sexton, 1990). Trd comprises well-defined bedding and small-scale depositional features such as laminations and ripple marks, but lacks well-defined, fining-upward sedimentary sequences, and contains less mudstone; interfingers with Trl and Tra.

Tra — **Ridge Route Formation, Apple Canyon Sandstone Member**—The Apple Canyon Sandstone member consists of yellowish-brown to olive-brown, fine- to medium-grained sandstone and silty sandstone interbedded with gray siltstone and shale (Swanson and Valencia, 2021). According to Sexton (1990), the ideal sequence for the Apple Canyon Sandstone Member is described as having massive to laminated, well-sorted, fine- to medium-grained sandstone with thin mudstone interbeds overlying a pebbly sandstone bed near the base. This member is commonly prone to block-glide landslide failures on dip-slopes (Sexton, 1990). This member reportedly contains freshwater mollusks, ostracodes, stromatolites, plant and vertebrate remains (Swanson and Valencia, 2021). Exposures of Apple Canyon Sandstone in the Liebre Mountain Quadrangle can be seen along Forest Service Road 8N01 near the western end of the quad (Sexton 1990).

Trc — **Ridge Route Formation, Cold Canyon conglomerate member**—Originally named by Faggioli (1952) as the Cold Canyon Formation for exposures along the south side of the Liebre Fault Zone, this unit has been adopted informally herein as the Cold Canyon conglomerate member of the Ridge Route Formation based on the description and relationship to the Ridge Route Formation as described by Faggioli; unit is extended southeast from Faggioli's study area as equivalent to "Trg" of Dibblee (2002). The Cold Canyon conglomerate consists primarily of yellowish-brown to light-brown, well-indurated, nonmarine cobble conglomerate and conglomeratic sandstone with a poorly sorted, silty, coarse angular-grained sandstone matrix. Resistant, continuous conglomerate beds were selectively mapped as marker beds within the unit based on interpretation from aerial imagery or lidar. A pinkish to reddish color occurs locally near the Liebre Fault zone. Locally micaceous, with biotite flakes commonly oxidized to a golden-brown. Near the Liebre Fault, cobble-size clasts are subrounded and composed of banded gneiss with minor amounts of aplite, dark-colored quartzites, orthoclase pegmatite, and meta-rhyolite (Faggioli, 1952); stromatolites locally abundant west of Knapp Ranch. Exposed as a discontinuous belt south of Liebre Fault from Cienega Canyon westward to Old Ridge Route. Farther south, Dibblee (2002) mapped a discontinuous conglomerate at the base and overlying conglomeratic sandstone; gradational contact with Tru; relationships with Trd unclear due to faulting.

Trp — **Ridge Route Formation, Piru Gorge Sandstone Member**—The Piru Gorge Sandstone contains a lower light gray (5Y 7/1) sandstone facies, fine-to locally coarse-grained, poorly bedded, with an organic-rich middle shale facies and thin interbeds of limestone, dolomite, chert, and siltstone; and an upper sandstone facies (modified from Link, 1982b). The shale facies contains plants, ostracodes and fish remains. The plant remains are indicative of deposition during late Miocene time (Link, 1982a).

Trff — **Ridge Route Formation, Frenchman Flat Sandstone Member**—Light yellowish- brown (2.5Y 6/3) medium-grained arkosic sandstone, gray (5Y 6/1) siltstone, and conglomerate, thin- to thick-bedded, well-cemented; low-angle cross-bedding plane-parallel laminations and ripple stratifications common. Ensley and Verosub (1982) report dates of 6.86 Ma near the base and 6.77 Ma near the top of this member.

Trfs — **Ridge Route Formation, Fisher Spring Sandstone Member**—Interbedded sandstone and siltstone strata of the Fisher Spring Member are exposed along Interstate 5 between Paradise Ranch and Whitaker Peak Road (Link, 1982a). Harper and Osborne (1982) divide the member into two sub-units based on depositional environment; only the upper unit is present within the map area. The upper unit is characterized by light-brown thick-bedded sandstone with a pronounced erosional basal contact with the underlying lacustrine facies and represents a fluvial deltaic sequence. Cross-bedding, soft-sediment slump folding, fining-upward sandstone channels, and shale rip-up clasts are common. Only a small area of the upper unit is present along the southern margin of the Liebre Mountain Quadrangle before transitioning northeastward into undifferentiated Ridge Route Formation. Ensley and Verosub (1982) report dates of 7.81 Ma near the base and 7.39 Ma near the top of this member based on magnetostratigraphic correlation.

Peace Valley Formation (late Miocene)—The Peace Valley Formation consists of fine-grained lacustrine sediments deposited along the axis of Ridge Basin and is exposed along the I-5 Freeway in the southwest portion of the map area. It is conformable and interfingers to the northeast, with the coarser-grained Ridge Route Formation. The Peace Valley Formation consists of five formal members distinguished either by intervening fingers of the Ridge Route Formation and/or by lithologic characteristics (Link, 1982a). The upper four members are exposed within the Liebre Mountain Quadrangle: Osito Canyon Shale, Cereza Peak Shale, Posey Canyon Shale, and Alamos Canyon Siltstone. Peace Valley "beds" were initially described by Crowell (1950), informally raised to formational status by Crowell (1964), and formalized by Dibblee (1967), as summarized by Link (1982a).

Tpa — **Peace Valley Formation, Alamos Canyon Siltstone Member**—The Alamos Canyon Siltstone member represents the uppermost section of the Peace Valley Formation; interfingers with Tra and Tru. It consists of olive-gray to gray shale, mudstone, and siltstone with local brown-weathering sandstone interbeds. The upper portion of the Alamos Canyon Siltstone contains a distinctive nonmarine fossil assemblage known as the Kinsey Ranch fauna (Miller and Downs, 1974), which indicates a late Miocene age of deposition.

Tppc — **Peace Valley Formation, Posey Canyon Shale Member**—The Posey Canyon shale consists of distinctive pale reddish-brown to gray, thinly bedded, argillite, soft mudstone, shale, pyritic siltstone and shale, and non-pyritic siltstone with local gypsum. The dominant argillite facies in this unit is unusual in Ridge Basin, in that it is composed primarily of analcime, ferroan dolomite, pyrite, and lesser amounts of quartz, feldspar, and illite, which is indicative of chemical sedimentation (Irvine, 1975). Fossil plants found in this member indicate a late Miocene age of deposition (Link 1982a).

Tpc — **Peace Valley Formation, Cereza Peak Shale Member**—Dark-gray shale and bluish-gray to pale-olive (5Y 6/3) and grayish-olive (10Y 4/2) mudstone with minor sandstone interbeds. Tpc is exposed in the southwest corner of the Liebre Mountain Quadrangle, along the I-5 Freeway. The Cereza Peak member contains mud cracks, wave ripples, Paleophycus trace fossils, fossil plants, ostracodes, and fish-remains; Ensley and Verosub (1982) report dates of 6.42 and 6.55 Ma in the upper portion of this unit based on magnetostratigraphic correlation.

Tpo — **Peace Valley Formation, Osito Canyon Shale Member**—Light-gray (2.5Y 6/1) to gray (5Y 6/1) shale and mudstone with interbeds of light-yellowish-brown (2.5Y 6/3) siltstone and sandstone. Shale contains minor carbonate and chert beds, ripple marks, burrow trace fossils, and animal tracks, but no megafossils; sandstone beds are both normally and inversely graded with cross bedding, ripple marks, shale rip-up clasts, and mud cracks (Link, 2003). Outcrops along the I-5 Freeway are friable with laminated to massive beds that form gentle hills with abundant vegetation growing on slope surfaces. Ensley and Verosub (1982) report dates of 7.34 Ma near the base and 6.94 Ma near the top of this member based on magnetostratigraphic correlation.

Tc — **Castaic Formation (late Miocene)**—Light- to dark-gray micaceous clay shale with thin interbeds of light-brown to brownish-gray arkosic sandstone interfinger with Tru along the southeastern portion of the Liebre Mountain Quadrangle. Soft-sediment deformation and dish structures in the sandstone interbeds are common. Basal section consists of pebbly sandstone tongues interfingering with fossiliferous marine shale; clasts consist chiefly of angular fragments of Proterozoic gneiss with some pebbles and cobbles reworked out of the San Francisquito Formation and rare Pelona Schist clasts. Megafossils recovered from the shale include *Turritella cooperi* and *Nemocardium centifilosum*, which suggest deposition during the Late Miocene in a marine embayment with water depths ranging from 50 to 90 m (Stanton, 1966). Shale dominates the formation with sandstone percentage and bed thickness increasing up-section, eventually grading into the overlying nonmarine Ridge Route Formation (Tru).

VOLCANIC ROCKS NORTHEAST OF SAN ANDREAS FAULT

Neenach Volcanics (Miocene to late Oligocene)—The Neenach Volcanics comprise a series of calc-alkaline andesitic, dacitic, and rhyolitic flows interbedded with pyroclastic and volcaniclastic sediments that were deposited unconformably onto Late Cretaceous quartz monzonite basement rock northeast of the San Andreas Fault within the Liebre Mountain Quadrangle. Mathews (1973b) subdivided the formation into eight distinct lithologic members, of which five are mapped within the Liebre Mountain Quadrangle.

Mathews (1973a; 1973b; 1976) interpreted that the Neenach Volcanics correlate across the San Andreas Fault with the Pinnacles Volcanics located in the central Coast Range near Soledad, California, based on striking similarities in geochemistry, petrography, stratigraphy, and age. This correlation has been widely cited to support about 315 km of right lateral separation on the San Andreas Fault since 23 Ma. However, field observations, unit relationships, and outcrop patterns observed in the making of this map and on adjacent quadrangles indicate that multiple units lie in depositional contact with the basement rock at different locations and locally occur in a different stratigraphic sequence than shown by Mathews (1973b; 1976). In addition, the volcanic units mapped by Mathews are laterally variable in thickness and likely interfinger and/or occur at more than one stratigraphic position based on observed outcrop patterns. Based on these relationships and observations, a revised, more complex correlation of map units is proposed for Neenach Volcanics, as shown in the correlation of map units for the Liebre Mountain Quadrangle.

Mathews (1973b) reported a K-Ar age of about 18 to 23 Ma for the Neenach Volcanics and Sims (1993) provided recalibrated ages of 19 to 24 Ma. These dates closely match K-Ar ages reported by Turner (1968) for the Pinnacles Volcanics. However, later Ar-Ar dating by Weigand and Swisher (1991) produced ages of about 12 and 14 Ma for the Neenach andesite (Tna) and dacite (Tnd) units, respectively, suggesting a discrepancy with the reported age of the Pinnacles Volcanics. New Ar-Ar dating of Neenach Volcanics units by the New Mexico Tech Geochronology Lab for CGS produced ages ranging from about 22 to 11 Ma (Matt Heizler written commun., 2022). The combination of the revised stratigraphic relationships and new Ar-Ar dating at the Neenach Volcanics suggest that additional studies are warranted to reassess the Neenach-Pinnacles Volcanics correlation.

Tnd — **Neenach Volcanics, dacite member**—Gray to pale-red dacite consisting of an aphanitic groundmass with white euhedral plagioclase, biotite and quartz phenocrysts; predominantly massive with local yellow, brown, and red color banding up to 2 to 3 cm thick. New Ar-Ar dating indicates an age of 14.37 +/-0.01 Ma (Matt Heizler written commun., 2023).

Tna — **Neenach Volcanics, andesite member**—According to Matthews (1976), Tna consists of four petrographic varieties: hypocrystalline hypersthene andesite, holocrystalline hypersthene andesite, augite-olivine andesite, and andesite tuff. Due to poor exposure, alteration, and faulting, these varieties are mapped as a single unit by Matthews (1976). The unit is poorly exposed in the map area and was inaccessible at the time of mapping. The hypocrystalline hypersthene andesite contains orthopyroxene, plagioclase, quartz, and rare clinopyroxene phenocrysts in a hyalopilitic groundmass. The holocrystalline hypersthene andesite consists of local phenocrysts of orthopyroxene and plagioclase in a plagioclase groundmass. The augite-olivine andesite contains abundant olivine and scattered clinopyroxene and plagioclase phenocrysts in a devitrified groundmass. (descriptions modified from Matthews, 1976). New Ar/Ar ages of 10.94 +/-0.05 Ma and 13.53 +/-0.05 Ma were obtained for this unit where mapped near Gorman (Matt Heizler written commun., 2022).

Tnpl — **Neenach Volcanics, pumice lapilli tuff member**—White to grayish-beige, and yellowish-green to grayish-green where altered, pumice lapilli tuff and tuff. Pumice fragments are up to 3 cm in maximum dimension, averaging 2 to 3 mm in diameter, and decreasing in diameter down-section. Angular fragments of flow-banded rhyolite from 1 to 3 mm in diameter are rare to abundant (Matthews, 1973b). Vaguely bedded with most beds less than 2 meters thick. Crystal fragments and lithic fragments/clasts from granitic basement rocks are abundant in the lower portion (modified from Olson and Swanson, 2019). Locally vesicular, with vesicles up to 1 mm in diameter. Texture varies from massive to chaotic, with brecciated lensoidal lapilli that are locally altered. Brecciated zones consist of green welded tuff clasts in a pink to purple matrix with local micro-brecciated lapilli. Unaltered zones of Tnpl are observable in the hills east of Sacombre Road in the adjacent Burnt Peak Quadrangle and are colored with yellowish residue on weathered minerals that give a speckled look in outcrop (Valencia and others, 2022). Small anhedral garnets up to 1 mm or less in diameter are disseminated in unaltered zones and are clustered adjacent to local quartz veins; lacking sanidine where analyzed.

Tnrp — **Neenach Volcanics, rhyolite member, perlite unit**—Black to brown-black, grayish-white to dusky greenish-gray, and tan to brown (where weathered) flow-banded perlite with alternating bands of clear and cloudy obsidian from 1 mm to 1.5 cm thick. Perlite is non-porphyritic with vitreous to waxy to resinous luster and inclusions of red, devitrified rhyolite (Matthews, 1976). Weathering occurs along foliation, jointing, and along quartz veins. Fractures conchoidally with sharp thin edges. Gradational and locally interfingered with map unit Tnrf. Unit is cut by many white to smoky quartz veins that display a range of translucent, semi-transparent to opaque properties. Micro-druzy quartz veins common. Characteristic outcrops are exposed along the north side of Pine Canyon Road across from Richardson Canyon.

Tnrf — **Neenach Volcanics, rhyolite member, flow-banded**—Pale-red, yellowish-gray, and grayish-purple (fresh), and white- to pale-yellowish-orange (weathered) aphanitic to fine-grained flow-banded rhyolite. Banding is continuous over several meters and defined by color variations. Bands are planar to locally undulatory or complexly folded during flow, ranging from <1 mm to >1 cm in thickness (Valencia and others, 2022). Outcrops can appear massive at a distance where flow bands are thin and pale. Bands of subrounded to subangular microbrecciated aphanitic rhyolite in fine-grained reddish-purple matrix are common. Soils on Tnrf slopes have abundant granule to pebble sized angular clasts and "popcorn" soil texture is common where outcrops are intensely weathered. New Ar-Ar dating near Three Points indicates an age of 22.07 +/-0.01 Ma (Matt Heizler written commun., 2023).

PALEOCENE TO LATE CRETACEOUS SEDIMENTARY ROCKS SOUTHWEST OF SAN ANDREAS FAULT

San Francisquito Formation (middle Palocene to Late Cretaceous)—The San Francisquito Formation consists of sediments deposited primarily in a deep-sea submarine fan system initiated during the Cretaceous to Paleocene time (Kooser, 1980). The oldest sediments are coarse grained and were deposited in shallow water (KTsfcs); as subsidence continued, sediments accumulated at the base of the continental slope (Tsfm) and in an adjacent submarine fan valley (Tsfc). Clasts in the basal conglomerate (KTsfcs) are dominantly composed of subangular to subrounded local granite and gneiss which suggest a local crystalline basement source terrain, whereas younger deep-water conglomerates (Tsfc) are well-rounded, polished, and contain abundant volcanic clasts, suggesting a more distant source with active silicic volcanism (Kooser, 1982; Olson and Valencia, 2021). Strata higher in the section were deposited on more distal portions of the fan in deeper water (Tsfs) as the marine transgression continued (Kooser, 1982). These units are located in the southeastern corner of the quadrangle and can be observed in exposed canyon walls.

Tsfc — **San Francisquito Formation, conglomerate (middle to early Paleocene)**—Dark-gray to brown, well-cemented cobbly to bouldery conglomerate with local, interleaved, medium- to thick-bedded, discontinuous sandstone beds, and rare mudstone. Conglomerates are commonly disorganized and clast-supported with beds up to 5 m thick. Clasts are typically polished and subrounded to well-rounded. Clast types include: quartz diorite, quartz monzonite, biotite-chlorite gneiss, quartzite, trachyandesite, porphyritic dacite and rhyodacite, devitrified crystal and lithic tuff, and sandstone intraclasts (Kooser, 1980; 1982). Sandstone beds are commonly medium-grained, lithic to arkosic, massive to parallel-laminated, and range in thickness from 10 to 50 cm. Equivalent to unit "KTsb" of Kooser (1980; 1982), which she infers was deposited in a deep-sea canyon near the apex of a submarine fan (Olson and Valencia, 2021). Tsfc interfingers with the mudstone member (Tsfm), such that the Tsfc overlies the Tsfm in the Liebre Mountain Quadrangle.

Tsfm — **San Francisquito Formation, mudstone (middle to early Paleocene)**—Very-dark-gray to dark-olive-brown silty mudstone, massive to thinly laminated, fissile, with finely disseminated carbonaceous debris, fossiliferous pebbly mudstone intervals, and common thin sandstone interbeds (Kooser, 1982). Interfingers laterally with Tsfc conglomerate in the Liebre Mountain Quadrangle. Equivalent to unit "KTsc" of Kooser (1980; 1982), which she infers was deposited at the base of the continental slope (Olson and Valencia, 2021).

Tsfs — **San Francisquito Formation, sandstone (middle to early Paleocene)**—Gray, light-grayish-brown, and light-brown, medium- to coarse-grained sandstone and pebbly sandstone with minor thin mudstone interbeds. Sandstone is medium- to thick-bedded with beds up to 3 m thick; locally crudely graded, and massive to parallel-laminated; cemented (Kooser, 1982). Equivalent to unit "Tsd" of Kooser (1980, 1982), which she infers was deposited in a submarine canyon extending across a submarine fan or as a suprafan lobe.

KTsfcs — **San Francisquito Formation, conglomerate and sandstone (early Paleocene to Late Cretaceous)**—A mixture of numerous shallow-water marine and perhaps some nonmarine facies. At maximum the unit is less than 100 m thick and in places pinches out entirely. Lithofacies include breccia, interstratified conglomerate and arenite, coal stringers, sandy-grainstone, biotite-wacke, and sandy-packstone to limy-arkosic wacke (Kooser, 1982). Unconformably overlies the gneissic and plutonic basement near the southeast corner of the Liebre Mountain quadrangle. Equivalent to "KTsa" unit of Kooser (1980; 1982) and considered to possibly include deposition in the Liebre Mountain area during Late Cretaceous time.

MESOZOIC INTRUSIVE ROCKS

Mesozoic intrusive rocks in the Liebre Mountain Quadrangle are separated into three groups by the San Andreas Fault (SAF). Quartz monzonite is mapped north of the fault and is thought to be related to the Sierra Nevada Batholith and generally older than the intrusive rocks south of the SAF (e.g. Nourse and others, 2020). Fine-grained granite occurs along and within the SAF Zone. Intrusive rocks also occur south of the fault and consist dominantly of Liebre granodiorite, quartz diorite, and subordinate granite, which are part of the Liebre Block of pre-SAF rocks as defined by Powell (1993) in the central Transverse Ranges. New U-Pb dating south of the SAF suggest that the Liebre granodiorite first started cooling at about 84 Ma followed by the quartz diorite around 77 to 76 Ma, and then the granite cooled last from about 76 to 73 Ma.

Kgr_1 — **Granite (Late Cretaceous)**—Dominantly very-light-gray to white, fine- to medium-grained, equigranular, massive to weakly foliated granite exposed within and immediately adjacent to the San Andreas Fault; locally ranges to medium- to coarse-grained and inequigranular; contains minor (<5%) fine-grained biotite. Exposures are weathered and occur east of Horse Camp Canyon along Pine Canyon Road and in sparse small natural outcrops, where fault movement has developed a fault gouge portion of the unit; mapped areas may include local overlying sandstone composed entirely of reworked granite debris. Age uncertain but presumed to be Late Cretaceous. Mapped initially by Barrows (1985).

Kgr_2 — **Granite (Late Cretaceous)**—Light-gray to pinkish-gray, fine- to medium-grained granite occurring as small pods southwest of the San Andreas Fault; likely related to small, local, fine-grained leucogranite dikes and other unmapped pods within older basement rocks; generally unfoliated to locally weakly foliated; mafic minerals compose <5% of rock. New U-Pb dating of the granite at two localities located in the adjacent Burnt Peak Quadrangle to the east produced Late Cretaceous ages of 76.3 +/-1.5 Ma and 73.1 +/-1.5 Ma (Valencia and others, 2022).

Kqd — **Quartz diorite (Late Cretaceous)**—Speckled, white and dark-gray to black, fine- to medium-grained, subequigranular biotite- and hornblende-bearing quartz diorite; biotite and hornblende commonly occur as small clots that are locally aligned to form a weak to moderate foliation; plagioclase is dominantly andesine in composition; locally includes granodiorite facies as observed near the east side of Liebre Mountain; is cut by local but widespread, Cretaceous, fine-grained, leucocratic granite dikes; includes intermixed diorite pods of varying size. Unit underlies much of Liebre Mountain and occurs along the southwest side of the Liebre Fault zone in the Liebre Mountain Quadrangle; contact with Liebre Granodiorite is poorly exposed. Unit is typically moderately coherent where exposed but commonly weathers to form sandy grus at the surface. Lithologically similar to quartz diorite on the Burnt Peak Quadrangle where it was informally named the "Warm Spring" diorite by Szatai (1961) and correlated by Dibblee (2002) with the Wilson Diorite of Miller (1934) in the southwestern San Gabriel Mountains; unpublished U-Pb dating of tonalitic rock of the Wilson diorite (LA-SF-ICPMS on zircons) indicates ages of 67 Ma and 73 Ma (J. Schwartz, CSUN Laser Lab, written commun., 2022). Previously unpublished U-Pb dating of a sample collected along Lake Hughes Road on the Burnt Peak Quadrangle to the east (Valencia and others, 2022) produced an age of 76.6 +/-1.5 Ma; granodioritic facies on the eastern part of Liebre Mountain in the Burnt Peak Quadrangle produced an age of 77.75 +/-0.59 [1.56] Ma (MSWD = 5.5) (ages +/-internal 2SE uncertainty [total 2% uncertainty]); analyses were conducted on zircons using laser ablation ICPMS analyses at the CSUN Laser Lab (J. Schwartz, written commun., 2022 and 2023).

Kli — **Liebre Granodiorite and Quartz Diorite (Late Cretaceous)**—Light-gray to gray biotite granodiorite and subordinate quartz diorite; originally designated by Crowell (1952) as Liebre Quartz Monzonite for exposures on the northwestern side of Liebre Mountain. This rock displays local weak foliation and is typically medium grained with hypidiomorphic, equigranular texture, but is locally coarse-grained or fine-grained with small subhedral phenocrysts of potassium feldspar (Sexton, 1990). Locally includes small, fine-grained leucocratic dikes, biotite schlieren, and intermixed small pods of diorite. The unit is exposed east of Ridge Basin and south of the San Andreas Fault and in the headwall of the Liebre and Bald Mountain Faults, where it is heavily overprinted by fracturing and minor faults, and commonly by landslide movement. Preliminary U-Pb cooling dates on zircon recently obtained by CGS for exposures in the Lebec Quadrangle to the northwest indicate ages between about 75 and 76 Ma. New dating of four samples of the granodiorite along Old Ridge Route in the Liebre Mountain Quadrangle indicate ages ranging from 80.75 +/-0.25 [1.62] to 83.73 +/-0.45 [1.67] Ma (age +/-internal 2SE uncertainty [total 2% uncertainty]); analyses were conducted on zircons using laser ablation ICPMS analyses at the CSUN Laser Lab (J.Schwartz, written commun., 2020). The new dating suggests the Liebre Granodiorite may have cooled between about 84 and 75 Ma, or that two periods of granodiorite emplacement occurred in the Bald/Liebre Mountain area; similarity in age of Liebre granodiorite obtained on the Lebec Quadrangle and intermixed quartz diorite similar to quartz diorite found at Liebre Mountain and along Lake Hughes Road suggests both units may be genetically related.

hd — **Hornblende diorite and gabbro (Mesozoic(?))**—Medium-gray, fine- to medium-grained hornblende diorite and local medium- to coarse-grained dark-gray to dark-greenish-gray gabbro with white plagioclase phenocrysts. Generally weathered and poorly exposed except in road cuts; forms local small pods and lenses. Age uncertain but may represent more than one phase of intrusion. A date of 81.73 +/-0.37 [1.63] Ma was obtained for the diorite facies; analyses were conducted on zircons using laser ablation ICPMS analyses at the CSUN Laser Lab (J.Schwartz, written commun., 2020).

Kqm — **Quartz monzonite (Late Cretaceous)**—Black and light-gray to white speckled, medium-grained to locally coarse-grained, massive to very weakly foliated quartz monzonite exposed north of the San Andreas Fault. Weathers to grus, forming rounded hills with rare natural exposures. Unit occurs extensively along the north side of the San Andreas Fault west of the Burnt Peak Quadrangle and north of Cookings Dry Lake. Previously unbublished U-Pb dating of quartz monzonite on the La Liebre Ranch Quadrangle to the northwest produced a preliminary early Late Cretaceous age of 92.1 +/-1.18 [1.84] Ma (age +/-internal 2SE uncertainty [total 2% uncertainty]); analyses were conducted on zircons using laser ablation ICPMS analyses at the CSUN Laser Lab (J.Schwartz, written commun., 2020).

Jggr — **Redrock Canyon granite (Jurassic?)**—Granite of probable Jurassic age intruded into the Ygn-p unit, forming a primary small plutonic body at Redrock Canyon and several small outlier bodies in the southeast portion of the map. Mapped by Smith (1951) as Jurassic granite, light-gray to reddish-brown weathering, porphyritic, leucocratic granite with K-feldspar phenocryst commonly ranging up to 1 cm in diameter in a fine-grained matrix. Commonly overprinted by pervasive fracturing or healed brecciation that is lined with reddish-brown, iron-oxide mineralization, which results in the namesake coloration in the type- location. Forms craggy outcrops, possibly due to secondary silicification.

Ꞧlm — **Liebre Mountain megaporphyry (Triassic)**—Megaporphyritic monzogranite/quartz monzonite with euhedral mega-phenocrysts of K-feldspar ranging from about 1.5 to 4 cm in length in a medium- to coarse-grained groundmass composed of plagioclase, K-feldspar, anhedral quartz, and mafic minerals including hornblende and subordinate biotite; Q-A-P ratio of 21-30-48; mega-phenocrysts contain inclusions of euhedral titanite, blebby to subhedral plagioclase, and irregular-shaped quartz; accessory minerals include titanite, apatite, epidote, zircon, and opaques (magnetite?) (abridged from Frizzell and others, 1986); locally overprinted by weak to moderate foliation. Frizzell and others (1986) reported an intrusive age of 215 Ma. Barth and Wooden (2006) obtained a revised, slightly older age of 250 +/- 3 Ma. New U-Pb dating of an exposure of the megaporphyry located near the San Andreas Fault and the Pacific Crest Trail (see location on map) produced an average age of 236.2 +/- 0.6 [4.7] Ma (MSWD = 4.7) (age +/-internal 2SE uncertainty [total 2% uncertainty]); analyses were conducted on zircons using laser ablation ICPMS analyses at the CSUN Laser Lab (J.Schwartz, written commun., 2020). This distinctive unit has been correlated with another megaporphyry intrusive unit north of the San Andreas Fault in the Mill Creek area of San Bernardino County, with nearly identical geochemistry, petrography, rubidium-strontium ratios, age of emplacement, and age of Late Cretaceous thermal overprinting, which has been interpreted to indicate about 160 km of total displacement on the Mojave strand of the San Andreas Fault (e.g. Matti and others, 1986; Frizzell and others, 1986).

PROTEROZOIC ROCKS

Prior mapping identified basement rock composed of gneiss and local marble of presumed Precambrian age exposed on the eastern portion of the Liebre Mountain Quadrangle (e.g. Dibblee, 2002), within the Liebre Mountain block of Powell (1993). The basement rocks of this block are separated from the Mendenhall Gneiss and other basement rocks of the southwestern San Gabriel Mountains by exposures of the Pelona Schist and the San Francisquito and Vincent Faults (not present in the map area). Szatai (1961) assigned the gneissic rock package in the Liebre Mountain and Burnt Peak areas to the informally named "Sawtooth Gneiss". Recent mapping on the Burnt Peak Quadrangle to the east distinguished two subunits that project into the Liebre Mountain Quadrangle, including an "Xgn_2" unit that included quartzofeldspathic, biotite and hornblende gneiss, and an "Xgn-p" unit that contains marble and quartzite layers that were interpreted to be meta-sedimentary in origin (Valencia and others, 2022). Initial U-Pb dating of zircons of the "Xgn_2" unit produced ages ranging from 1.72 to 1.80 Ga (Valencia and others, 2022), similar to the reported age of the Mendenhall Gneiss (e.g. Barth and others, 2001). Subsequent U-Pb dating of the "Xgn-p (m)" unit produced a much younger zircon age of about 1.17 Ga (Swanson and others, 2023).

Ygn-p — **Quartzofeldspathic paragneiss with marble (early Paleozoic(?) to Mesoproterozoic)**—Light-brown weathering quartz- and feldspar-rich gneiss with small, oxidized biotite or hornblende grains, which includes discontinuous bands of light-gray to white marble ranging up to about 8 m in thickness and thin, light-gray quartzite beds, which substantiates the paragneiss interpretation; locally contains well-rounded quartz grains, pebbles, cobbles, and sandy layers exhibiting primary bedding (Szatai, 1961). The gneiss is moderately foliated, defined by mm- to cm-scale bands of varying grain size and quartz content; foliation is generally planar with few observed small-scale folds; weakly fissile but generally fractured and weathered, forming few exposures except in road cuts and channel banks, and at larger marble beds. Contact with older Xgn gneiss is subtle, but presumably was originally an unconformity, which is now overturned with a dominantly south vergence in most areas based on observed structural relationships. Unit is intruded by granite of Redrock Canyon and smaller Kgr pods; unconformably overlain by the San Francisquito Formation and the Ridge Route Formation. Previously unpublished U-Pb dating of zircons from the adjacent Burnt Peak quadrangle (Valencia and others, 2022) produced an upper intercept age of 1,174 +/-22.9 [23.5] Ma (MSWD = 2.0) (age +/-internal 2SE uncertainty [total 2% uncertainty]); analyses were conducted on zircons using laser ablation ICPMS analyses at the CSUN Laser Lab (J.Schwartz, written commun., 2023). The dated zircons are presumably detrital and therefore the unit is younger than 1.17 Ga, and therefore could be Mesoproterozoic, Neoproterozoic, or even early Paleozoic in age (labeled as Ygn-p for the Liebre Mountain quadrangle based on new U-Pb age), followed by subsequent metamorphism.

m — **Marble**—Light-gray to white marble subunits of Ygn-p that are sufficiently large to map; generally fine-grained with mm- to cm-scale banding that locally represents original bedding; locally coarsely recrystallized; disseminated graphite is also commonly present.

Xgn — **Quartzofeldspathic gneiss (Paleoproterozoic)**—Undifferentiated gneiss consisting primarily of quartzofeldspathic gneiss with local biotite gneiss, hornblende gneiss, and local lenses of amphibolite; gneiss subunits are not differentiated on map due to poor lateral exposure of contacts. The quartzofeldspathic gneisses generally contain only minor mafic minerals and consist of two primary lithologies; gneiss observed in the Cienega Canyon area is dominantly fine-to medium-grained and displays cm-scale, light- to medium-gray foliation bands with poor fissility; gneiss exposed in the Fish Canyon area is dominantly pinkish gray and weakly foliated, also with poor fissility and is cut by numerous leucocratic granitic dikes. Previously unpublished U-Pb dating on zircons from similar pinkish-gray gneiss on the Burnt Peak quadrangle (Valencia and others, 2022) produced an age of 1,796.5 +/-9.8 [35.9] Ma (MSWD = 1.7) (age +/-internal 2SE uncertainty [total 2% uncertainty]); analyses were conducted on zircons using laser ablation ICPMS analyses at the CSUN Laser Lab (J.Schwartz, written commun., 2023). Unit is generally fractured overall; best exposed in channel banks and deeply incised canyon slopes in the Fish Creek and Cienega Canyon tributary watersheds. Locally intruded by granite bodies and numerous leucocratic granitic dikes of uncertain affinity in the Fish Canyon area. Quartzofeldspathic gneisses are likely orthogneiss. Local presence of hornblende suggests amphibolite grade metamorphism.

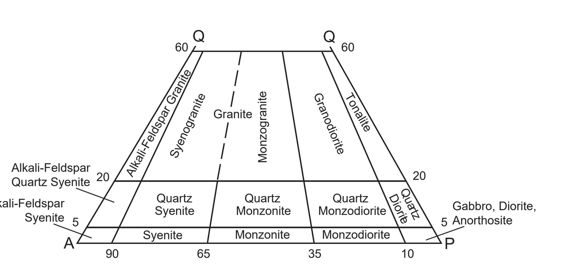

Classification of plutonic rock types (from Streckeisen, 1973; 1976).
A, alkali feldspar; P, plagioclase feldspar; Q, quartz.

CORRELATION OF MAP UNITS

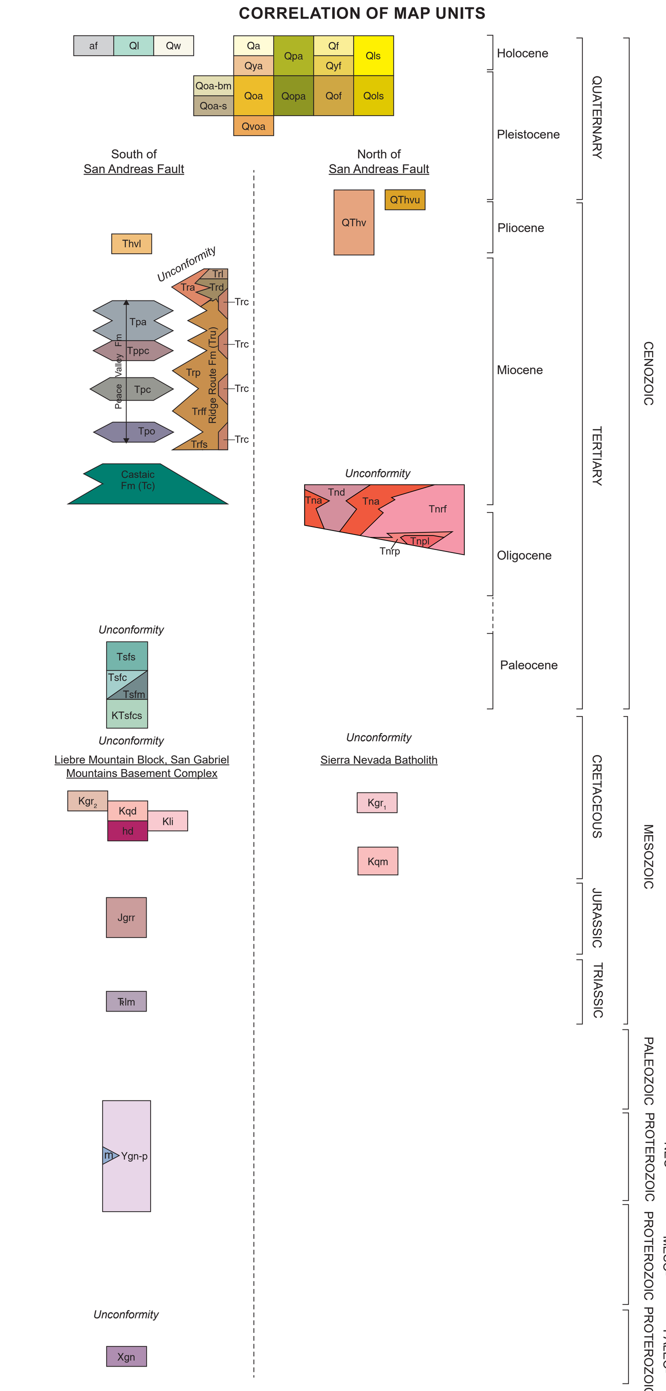

MAP SYMBOLS

Contact between map units—Solid where accurately located; long dash were approximately located; short dash where inferred; dotted where concealed; queried where identity or existence is uncertain

Fault—Solid where accurately located; long dash were approximately located; short dash where inferred; dotted where concealed; queried where identity or existence is uncertain. Arrow and number indicate direction and angle of dip of fault plane. Faults labeled in quotations are informal names from Sexton (1990): "Campground fault" named after Tumble Inn Campground, and "West Lookout fault" named after West Liebre Lookout; and from Szatai (1961): "Bear Canyon fault" named after Bear Canyon.

Thrust Fault—Barbs on upper plate; solid where accurately located; long dash where approximately located; dotted where concealed; queried where identify or existence is uncertain. Arrow and number indicate direction and angle of dip of fault plane

Syncline (sedimentary rock) or synform (gneiss)—Solid where accurately located, long dash where approximately located, dotted where concealed; queried where identity or existence is uncertain; arrow showing plunge direction

Anticline—Solid where accurately located, long dash where approximately located, dotted where concealed; queried where identity or existence is uncertain; arrow showing plunge direction

Transition along strike between formal members and undifferentiated strata of Ridge Route Formation

Dike

Sandstone Marker Bed—Interpreted from aerial imagery or lidar

Conglomerate Marker Bed—Interpreted from aerial imagery or lidar

Landslide—Arrows indicate principal direction of movement. Where mapped as a landslide complex, adjacent defined slides have different relative ages and/or failure types.

U-Pb Geochronology point (six samples)

IRSL Geochronology point (one sample)

Stromatolite Fossil Locality

Area of mine-related ground disturbance

Strike and dip of geologic structure; number indicates dip angle in degrees; attitudes lacking dip numbers are approximate attitudes obtained from Dibblee and Minch (2002).

25 Bedding	50 Metamorphic foliation
70 Approximate bedding	Vertical metamorphic foliation
85 Overturned bedding	75 Minor fault orientation
40 Igneous foliation	60 Shear

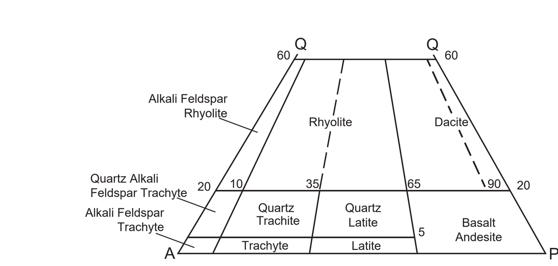

QAPF modal classification of volcanic rock types (based on Le Maitre, 2002).
This diagram must not be used for rocks in which the mafic mineral content, M, is greater than 90%.
A, alkali feldspar; P, plagioclase feldspar; Q, quartz

SELECTED REFERENCES

Barrows, A.G., Kahle, J.E., and Beeby, D.J., 1985, Earthquake hazards and tectonic history of the San Andreas Fault Zone, Los Angeles County, California: California Division of Mines and Geology, Open File Report 85-10LA, 139 p, Plate 1a, scale 1:12,000.

Barth, A.P., Wooden, J.L., and Coleman, D.S., 2001, SHRIMP-RG U-Pb zircon geochronology of Mesoproterozoic metamorphism and plutonism in the southwesternmost United States: Journal of Geology, v. 109, p. 319-327.

Barth, A.P., and Wooden, J.L., 2006, Timing of magmatism following initial convergence at a passive margin, southwestern U.S. Cordillera, and ages of lower crustal magma sources: Journal of Geology, v. 114, p.231-245.

Crowell, J.C., 1950, Geology of the Hungry Valley area, southern California: Bulletin of the American Association of Petroleum Geologists, v. 34, no. 8, p. 1623-1646.

Crowell, J.C., 1964, The San Andreas Fault zone from the Temblor Mountains to the Antelope Valley, southern California: American Association of Petroleum Geologists, Society of Economic Paleontologists and Mineralogists, Pacific Sections, and San Joaquin Geological Society Guidebook, p. 1-39.

Crowell, J.C., 1982, Geologic Map of Ridge Basin, *in* Crowell, J. C., and Link, M. H., eds., Geologic History of Ridge Basin, southern California: Pacific Section, Society of Economic Paleontologists and Mineralogists, Field Trip Guidebook and Volume, Plate 1 and 2, scale 1:24,000.

Crowell, J.C., (and others), 2002, Geologic map of Ridge Basin, southern California, *in* Crowell, J. C., ed., 2003, Evolution of Ridge Basin, southern California: An interplay of sedimentation and tectonics: Geological Society of America Special Paper 367, Plate I, scale about 1:51,375.

Crowell, J.C., 2003a, Overview of rocks bordering Ridge Basin, southern California, in Crowell, J. C., ed., Evolution of Ridge Basin, southern California: An interplay of sedimentation and tectonics: Geological Society of America Special Paper 367, p. 89-112.

Crowell, J.C., 2003b, Introduction to geology of Ridge Basin, southern California, *in* Crowell, J. C., ed., Evolution of Ridge Basin, southern California: An interplay of sedimentation and tectonics: Geological Society of America Special Paper 367, p. 1-15.

Crowell, J.C., 2003c, Tectonics of Ridge Basin region, southern California, *in* Crowell, J. C., ed., Evolution of Ridge Basin, southern California: An interplay of sedimentation and tectonics: Geological Society of America Special Paper 367, p. 157-203.

Dibblee, T.W. Jr., 1967, Areal geology of the western Mojave Desert, California: U.S. Geological Survey Professional Paper 522, 153 p.

Dibblee, T.W. Jr., and Minch, J.A., 2002, Geologic map of the Liebre Mountain quadrangle, Los Angeles County, California: Dibblee Geological Foundation, Dibblee Foundation Map DF-93, scale 1:24,000

Ehman, K.D., Sullivan, M.D., and May, S.R., 2000, Ridge Basin field trip guidebook - Tectonic controls on facies distribution and stacking patterns, Ridge Basin, southern California: Pacific Section SEPM, Book 87, 50 p.

Ensley, R.A., and Verosub, K.L., 1982, Biostratigraphy and magnetostratigraphy of southern Ridge Basin, central Transverse Ranges, California, *in* Crowell, J.C., and Link, M.H., eds., Geologic History of Ridge Basin, southern California: Pacific Section, Society of Economic Paleontologists and Mineralogists, Field Trip Guidebook and Volume, p. 13-24.

Faggioli, R.E., 1952, The geology of the Liebre Fault, California: Master's thesis, University of California, Los Angeles, 56 p., Plate 3, scale 1:12,000.

Foster, B.D., 2003, Landslides in the Interstate 5 corridor between Valencia and Gorman, Los Angeles County, California: California Geological Survey, Special Report 188, 23 p.

Frizzell, V.A., Jr., Mattinson, J.M., and Matti, J.C., 1986, Distinctive Triassic megaporphyritic monzogranite: Evidence for only 160 km of offset along the San Andreas Fault, southern California: Journal of Geophysical Research, v. 91, no. B14, p. 14,080-14088.

Harper, A.S., and Osborne, R.H., 1982, Fluviolacustrine facies of the Fisher Spring Sandstone Member, Mio-Pliocene Ridge Route Formation, Ridge Basin, southern California, *in* Crowell, J. C., and Link, M. H., eds., Geologic History of Ridge Basin, southern California: Pacific Section, Society of Economic Paleontologists and Mineralogists, Field Trip Guidebook and Volume, p. 105-114.

Irvine, P.J., 1975, The Posey Canyon Shale: A Pliocene lacustrine deposit of the Ridge Basin, southern California: Unpublished Master's Thesis, University of California, Berkeley (Occidental College), 87 p.

Jennings, C.W., 1953, Geology of the southern part of the Quail Quadrangle, California: Department of Natural Resources, Division of Mines, Special Report 30, 18 p., Plate 1, scale 1:24,000.

Kooser, M.A., 1980, Stratigraphy and Sedimentology of the San Francisquito Formation, Transverse Ranges, California: Unpublished doctoral dissertation, University of California, Riverside, 201 p, Plate I, scale 1:24,000.

Kooser, M.A., 1982, Stratigraphy and sedimentology of the type San Francisquito Formation, southern California, *in* Crowell, J.C., and Link, M.H., eds., Geologic history of Ridge Basin, southern California: Pacific Section, Society of Economic Paleontologists and Mineralogists, p. 53-61.

Lancaster, J.T., Hernandez, J.L., Haydon, W.D., Dawson, T.E., and Hayhurst, C.A., 2012, Geologic Map of Quaternary Surficial Deposits, Lancaster 30' X 60' Quadrangle, *in* Bedrossian, T.L., Roffers, P.D., Hayhurst, C.A., Lancaster, J.T., and Short, W.R., compilers, Geologic compilation of Quaternary surficial deposits in southern California: California Geological Survey, Special Report 217, Plate 22, scale 1:100,000.

Le Maitre, R.W., 2002, Igneous Rocks: A classification and glossary of terms: Recommendations of the International Union of Geological Sciences, Sub commission on the Systematics of Igneous Rocks: International Union of Geological Sciences, eBook.

Link, M.H., 1978, Lacustrine stromatolites and associated sediments of the Pliocene Ridge Route Formation, Ridge Basin, California: Journal of Sedimentary Petrology, v. 48, no. 1, p. 143-158.

Link, M.H., 1982a, Stratigraphic nomenclature and age of Miocene strata, Ridge Basin, southern California, *in* Crowell, J. C., and Link, M.H., eds., Geologic History of Ridge Basin, southern California: Pacific Section, Society of Economic Paleontologists and Mineralogists, Field Trip Guidebook and Volume, p. 5-12.

Link, M.H., 1982b, Introduction to the facies of the Ridge Route Formation, Ridge Basin, southern California, *in* Crowell, J. C., and Link, M.H., eds., Geologic History of Ridge Basin, southern California: Pacific Section, Society of Economic Paleontologists and Mineralogists, Field Trip Guidebook and Volume, p. 99-104.

Link, M.H., 1982c, Provenance, paleocurrents, and paleogeography of Ridge Basin, southern California, *in* Crowell, J. C., and Link, M.H., eds., Geologic History of Ridge Basin, southern California: Pacific Section, Society of Economic Paleontologists and Mineralogists, Field Trip Guidebook and Volume, p. 265-275.

Link, M.H., 1983, Sedimentation, tectonics, and offset of Miocene-Pliocene Ridge Basin, California, *in* Anderson, D.W., and Rymer, M.J., eds., Tectonics and sedimentation along faults of the San Andreas system: Pacific Section Society of Economic Paleontologists and Mineralogists Volume, p. 17-31.

Link, M.H., 2003, Depositional systems and sedimentary facies of the Miocene-Pliocene Ridge Basin Group, Ridge Basin, southern California, *in* Crowell, J.C., ed., Evolution of Ridge Basin, southern California: An interplay of sedimentation and tectonics: Geological Society of America, Special Paper 367, p. 17-87.

Loeffler, R.D., and Bennett, J.D., 1990, Lower member deposition, Hungry Valley Formation, Los Angeles and Ventura Counties: California Geology, August issue, v. 43, no. 8, p. 178-184.

Mathews, V., III, 1973a, Pinnacles-Neenach correlation: A restriction for models of the origin of the Transverse Ranges and the Big Bend in the San Andreas Fault: Geological Society of America, Bulletin, v. 84, no. 2, p. 683-688.

Mathews, V., III, 1973b, Geology of the Pinnacles Volcanic Formation and Neenach Volcanic Formation and their bearing on the San Andreas Fault problem: Unpublished Doctoral Thesis, University of California, Santa Cruz, 214 p, Plate 2, scale 1:24,000.

Mathews, V., III, 1976, Correlation of Pinnacles and Neenach Volcanic Formations and their bearing on San Andreas Fault problem: American Association of Petroleum Geologists, Bulletin, v. 60, no. 12, p. 2128-2141.

Matti, J.C., Frizzell, V.A., and Mattinson, J.M., 1986, Distinctive Triassic megaporphyritic monzogranite displaced 160 +/-10 km by the San Andreas Fault, southern California: A new constraint for palinspastic reconstructions: Geological Society of America Abstracts with Programs, v. 18, p. 154.

Miller, W.J., 1934, Geology of the western San Gabriel Mountains of California: University of California, Los Angeles, Publications in Mathematical and Physical Sciences, v. 1, no. 1, 113 p.

Munsell Color Co., Inc., 2019, Munsell soil-color charts (2009 revised ed.): Grand Rapids, Michigan.

Nourse, J.A., Swanson, B.J., Lusk, A.D., Barth, N.C., Schwartz, J.J., and Vermillion, K.B., 2020, Recent advancements in geochronology, geologic mapping, and landslide characterization in basement rocks of the San Gabriel Mountains block, *in* Heermance, R.V., and Schwartz, J.J., eds. From the Islands to the Mountains: A 2020 View of Geologic Excursions in Southern California: Geological Society of America Field Guide 59, p. 21–93, https://doi.org/10.1130/2020.0059(02).

Olson, B.P.E., and Swanson, B.J., 2019, Preliminary geologic map of the La Liebre Ranch Quadrangle, Kern and Los Angeles, counties, California: California Geological Survey, Preliminary Geologic Map 19-03, Version 1.0, map scale 1:24,000

Olson, B.P.E., and Valencia, F.N., 2021, Preliminary geologic map of the Whitaker Peak Quadrangle, Kern and Los Angeles, counties, California: California Geological Survey, Preliminary Geologic Map 21-03, Version 1.0, map scale 1:24,000.

Powell, R.E., 1993, Balanced palinspastic reconstruction of pre-late Cenozoic paleogeology, southern California: Geologic and kinematic constraints on evolution of the San Andreas Fault system, *in* Powell, R.E., Weldon, R.J., II, and Matti, J.C., eds., The San Andreas Fault system—displacement, palinspastic reconstruction, and geologic evolution: Geological Society of America, Memoir 178, Chapter 1, p. 1-106.

Ross, D.C., 1969, Map showing recently active breaks among the San Andreas Fault between Tejon Pass and Cajon Pass, southern California: U. S. Geological Survey, Miscellaneous Investigations Series, Map I-553, scale 1:24,000.

Rust, D.J., 1985, Geologic, geomorphic, and structural analysis of Quaternary tectonic behavior: San Andreas fault zone in the Transverse Ranges north of Los Angeles, California: Unpublished Doctoral Thesis, University of California, Santa Barbara, 478 p, Plate 1 – West Half, scale 1:12,000.

Sexton, C.J., 1990, Geologic Structure of the Liebre Fault Zone south of Bald Mountain, northern Los Angeles County, California: Unpublished Master's Thesis, California State University, Los Angeles, 123 p, Plate I, scale 1:12,000.

Sims, J.D., 1993, Chronology of displacement on the San Andreas Fault in central California: Evidence from reversed positions of exotic rock bodies near Parkfield, California, in Powell, R.E., Weldon, R.J., II, and Matti, J.C., eds., The San Andreas Fault system—displacement, palinspastic reconstruction, and geologic evolution: Geological Society of America, Memoir 178, Chapter 1, p. 231-256.

Smith, D. 1980, Fault Evaluation Report: San Andreas Fault, Liebre Mountain Quadrangle, Los Angeles County: California Division of Mines and Geology, Fault Evaluation Report FER-75, p. 1-4.

Smith, V.M., 1951, Geology of the upper Castaic Creek region, Los Angeles County, California: Unpublished Master's Thesis, University of California, Los Angeles, 31 p., Plate VI, scale 1:24,000.

Streckeisen, A.L., 1973, Plutonic rocks—Classification and nomenclature recommended by the IUGS Sub Commission on Systematics of Igneous Rocks: Geotimes, v.18, p. 26–30.

Streckeisen, A.L., 1976, To each plutonic rock a proper name: Earth Science Reviews, v. 12, p. 1–33.

Swanson, B.J., and Valencia, F.N., 2021, Preliminary geologic map of the Black Mountain 7.5′ Quadrangle, Los Angeles and Ventura counties, California: California Geological Survey, Preliminary Geologic Map 21-02, scale 1:24,000.

Swanson, B.J., Valencia, F.N., and Hernandez, J.L., 2023, New insights on the age, distribution, and structure of basement rocks on the southwest side of the San Andreas Fault in the Burnt Peak 7.5' Quadrangle, southern California: Geological Society of America Abstract and Poster, Cordilleran Section Meeting, Reno Nevada.

Szatai, J.E., 1961, The geology of parts of the Redrock Mountain, Warm Spring, Violin Canyon, and Red Mountain Quadrangles, Los Angeles County, California [dissertation]: University of Southern California, 164 p., Plate 1, scale 1:24,000.

Turner, D.L., 1968, Potassium argon dates concerning the Tertiary foraminiferal time scale and San Andreas Fault displacement: Unpublished PhD Thesis, University of California, Berkeley, 99 p.

Valencia, F.N., Swanson, B.J., and Hernandez, J.L. 2022, Preliminary geologic map of the Burnt Peak 7.5′ Quadrangle, Los Angeles County, California: California Geological Survey, Preliminary Geologic Map 22-06, scale 1:24,000.

Weber, F.H., Jr., 1988, Evaluation of activity of the San Gabriel Fault Zone, Los Angeles and Ventura Counties, California: Final Technical Report, Part I of V, USGS Contract Number 14-08-0001-21928, 161 p., map scale: 1:12,000.

Weigand, P.W., and Swisher, C.C., III, 1991, Are the Neenach and Pinnacles Volcanic Formations miscorrelated? New evidence from 40Ar/39Ar dating: EOS, v. 72, no. 44, p. 577.

Weldon, R.J., Meisling, K.E., and Alexander, J., 1993, A speculative history of the San Andreas Fault in the central Transverse Ranges, California, *in* Powell, R.E., Weldon, R.J., II, and Matti, J.C., eds., The San Andreas Fault system—displacement, palinspastic reconstruction, and geologic evolution: Geological Society of America, Memoir 178, Chapter 1, p. 161-198.

Wood, M.F., 1981, Depositional environments of the Apple Canyon sandstone, Ridge Basin, central Transverse Range, California: Unpublished Master's Thesis, University of Southern California, 266 p, Plate 1, scale 1:24,000.

Wood, M.F., and Osborne, R.H., 1982, Sedimentology of the Mio-Pliocene Apple Canyon Sandstone Member, Ridge Route Formation, Ridge Basin, southern California, *in* Crowell, J. C., and Link, M. H., eds., Geologic History of Ridge Basin, southern California: Pacific Section, Society of Economic Paleontologists and Mineralogists, Field Trip Guidebook and Volume, p. 135-142.

IMAGERY

Google Earth Pro, 2022, Color and Black & White imagery dated between April 2015 and April 2017.

Lidar 1 m DEM: B4 Project - Southern San Andreas and San Jacinto Faults. Distributed by OpenTopography. https://doi.org/10.5069/G97P8W9T . Accessed: 2023-07-21

OCM Partners, 2017: 2015 - 2016 LARIAC Lidar DEM: Los Angeles Region, CA, https://www.fisheries.noaa.gov/inport/item/55257.

U.S. Department of Agriculture, 2005, Farm Service Agency–Aerial Photography Field Office, National Agriculture Imagery Program (NAIP), 1 meter, resolution. http://datagateway.nrcs.usda.gov/

U.S. Department of Agriculture, 2020, Farm Service Agency–Aerial Photography Field Office, National Agriculture Imagery Program (NAIP), 60cm, resolution. http://datagateway.nrcs.usda.gov/

Suggested citation:
Rodriguez, F.N. and Swanson, B.J., 2023, Preliminary geologic map of the Liebre Mountain 7.5′ Quadrangle, Los Angeles County, California: California Geological Survey Preliminary Geologic Map 23-02, scale 1:24,000.

AUTHORSHIP DOCUMENTATION AND PRODUCT LIMITATIONS

PUBLICATION TITLE: Preliminary Geologic Map of the Liebre Mountain 7.5’ Quadrangle, Los Angeles County, California
Preliminary Geologic Map 23-02

LIMITATIONS: This map is considered preliminary, and the California Department of Conservation makes no warranties as to the suitability of this product for any given purpose. This map should not be considered as an authoritative or comprehensive source for landslide and seismic hazard data. For landslide data, please visit the California Geological Survey Landslides web page at: **https://www.conservation.ca.gov/cgs/landslides**. For seismic hazards data and Zones of Required Investigation, please visit the California Geological Survey Seismic Hazards Program web page at: **https://www.conservation.ca.gov/cgs/sh/program**.

First Author – Francesca N. Rodriguez, PG 10171

Date: September 26, 2023

PROFESSIONAL GEOLOGIST
Francesca N.
Rodriguez
No. 10171
STATE OF CALIFORNIA

Second Author – Brian J. Swanson PG 6494, CEG 2055

Date: September 26, 2023

CERTIFIED ENGINEERING GEOLOGIST
Brian J.
Swanson
No. 2055
STATE OF CALIFORNIA

This authorship document accompanies the geologic map with the following citation:

Rodriguez, F.N. and Swanson, B.J., 2023, Preliminary geologic map of the Liebre Mountain 7.5’ Quadrangle, Los Angeles County, California: California Geological Survey Preliminary Geologic Map 23-02, scale 1:24,000.